Available online at www.sciencedirect.com
ScienceDirect
Cement and Concrete Research 37 (2007) 671–679
Cement and Concrete Research

An XRD study of the effect of the SiO_2/Na_2O ratio on the alkali activation of fly ash

M. Criado [a], A. Fernández-Jiménez [a,*], A.G. de la Torre [b], M.A.G. Aranda [b], A. Palomo [a]

[a] *Eduardo Torroja Institute (CSIC), c/ Serrano Galvache, no. 4, 28033 Madrid, Spain*
[b] *Department of Inorganic Chemistry, University of Málaga, Campus Teations s/n, 29071 Málaga, Spain*

Received 13 November 2006; accepted 26 January 2007

Abstract

Soluble silica has a very significant effect on the microstructural and mechanical development of the cementitious materials produced as a result of the alkali activation of fly ash. In this study, four different alkaline solutions with different soluble silica contents were used to activate fly ash. The primary reaction product was a sodium aluminosilicate gel, while different types of zeolites appeared as minority phases. The percentage and composition of these reaction products were found to depend on both the soluble silica content present in the activating solutions and the thermal curing time. In addition, the amount of gel was observed to have a decisive effect on the mechanical strength developing in the material.

Keywords: Fly ash; Rietveld method; Silicate–sodium oxide ratio

1. Introduction

In 1959, V.D. Glukhovshy [1] suggested that the construction industry could benefit from the use of what he called "soil cements", new cementitious products resulting from attacking certain (natural or industrial waste) aluminosiliceous materials with alkaline salt solutions. The fly ash produced in steam power plants is one such aluminosilicate suitable for alkali activation [2].

Although the mechanisms that regulate the reactions between alkaline activator and fly ash are not fully understood, the models that are gradually being developed afford a fairly precise view of what actually takes place [3,4]. The activation rate and chemical composition of the reaction products depend on factors such as ash particle size and chemical composition, type and concentration of the activator, etc. Nonetheless, the mechanisms that control the general activation process are independent of the values assumed by these variables at any given time. The above findings informed the decision to conduct the present study on the effect of the soluble silica content in the activating solution on the reaction rate of the "ash-activator" system and the nature of the reaction products. Prior research [5–7] had shown that the H_2O/SiO_2 and OH^-/SiO_2 ratios have a considerable impact on the "molecular" or "polymeric" species present in the reaction mix and the rate of uptake of these species into the three-dimensional structure of the tectosilicates.

The main reaction product of the alkali activation of fly ash is a sodium aluminosilicate gel. This amorphous material has hitherto been very difficult to characterize, but the understanding of its structure and composition is growing steadily more precise with the increasingly powerful analytical techniques now deployed. According to NMR findings, it does, however, exhibit short-range order, with a three-dimensional structure in which silicon is found in a variety of environments, $Q^4(nAl)$: on this basis, the gel can be regarded to be a "*zeolite precursor*" [4].

Rietveld methodology consists on the comparison between the measured and calculated powder diffraction patterns. The analysis of the whole pattern minimises the inaccuracies derived of systematic errors inside the raw data such as peaks overlap, preferred orientation(s), peak broadening and lack of a pure standard(s).The Rietveld method is a powerful tool to successfully carry out quantitative phase analysis (QPA) of

* Corresponding author.
E-mail address: pesfj18@ietcc.csic.es (A. Fernández-Jiménez).

0008-8846/$ - see front matter © 2007 Elsevier Ltd. All rights reserved.
doi:10.1016/j.cemconres.2007.01.013

Table 1
Elemental composition of Compostilla fly ash, expressed as oxides (%)

SiO_2	Al_2O_3	Fe_2O_3	CaO	MgO	SO_3	Na_2O	K_2O	TiO_2	L.O.I[a]	IR[b]	Total
53.09	24.80	8.01	2.44	1.94	0.23	0.73	3.78	1.07	3.59	0.32	100.00

[a]L.O.I. loss on ignition; [b]IR insoluble residue.

crystalline complex systems [8–13] although the crystal structures of all crystalline phases must be known. This methodology is also suited to follow structural changes [14,15] due to different elemental composition. Moreover, the Rietveld methodology has also been extended to indirectly determine the amorphous content in a given crystalline sample by adding a suitable standard [16].

The aim of the present study was to explore the effect of the soluble silica content in a series of activating solutions on the microstructural development of "ash-activator" system reaction products, and to identify and quantify such products and their impact on mechanical development in the material.

2. Experimental

2.1. Characterization of initial materials

A type F (as defined in ASTM standard C6128–03) fly ash from the Compostilla steam power plant in Spain, consisting primarily of SiO_2 and Al_2O_3 was used in the present study. The chemical composition of the ash (determined as described in Spanish standard UNE 80–230–99) and percentage of reactive silica (established following the procedure set out in Spanish standard UNE 80–225–93) are shown in Tables 1 and 2, respectively. Ninety two per cent of the particles in this ash were <45 μm [17].

The ash was activated with a series of alkaline solutions, all with a practically constant sodium oxide content (≈ 8%), but with varying proportions of soluble silica. The products used to prepare the solutions were laboratory reagents: ACS-ISO 98% pure NaOH pellets supplied by Panreac S.A. and sodium silicate with a density of 1.38 g/cc with the following composition: 8.2% Na_2O; 27% SiO_2 and 64.8% H_2O. The chemical composition and certain other properties of each solution are given in Table 3, which also shows the differences in both the silica and the water content achieved by mixing sodium silicate and sodium hydroxide in different proportions.

2.2. Methodology

2.2.1. Alkali activation of fly ash

The ash was mixed with the activating solutions described in Table 3 to prepare prismatic paste specimens (1 × 1 × 6 cm). The "solution/ash" ratio used was 0.4 by weight. Specimens were cured at 85 °C for: 8 h, 7, 28, 60, 90 or 180 days. The humidity was kept at >90% at all times. The activated ash specimens were subjected to standard cement strength tests (as per European code EN 196–1) at the different reaction times (12 prisms per test were tested).

After each experiment, the material was grinded (size<65 μ) and mixed with a small volume of acetone in order to dehydrate the system and then to prevent the material evolution.

2.2.2. Determination of the percentage of reaction products

The hardened pastes were attacked with 1:20 HCl (by volume) to determine the percentage of reaction products generated at the respective reaction times (the HCl used to prepare the solutions 1:20 was hydrochloric acid 37% PA-ACS-ISO). This procedure separates the reaction products (sodium aluminosilicate gel and zeolites) which are dissolved in the acid, from the unreacted ash, which remains in the insoluble residue [18,19]. The dissolved fraction is a parameter that provides information on the conversion factor α, i.e., how far the reaction has progressed.

The experimental process followed consisted on placing 1 g of the ground (to a powder, particle size<65 μm) hardened material (activated ash) in a 250-ml flask containing 1:20 HCl. The mix was stirred with a plastic rotor for 3 h, after which it was filtered (through filter paper with a pore size of 15–20 μm) and the insoluble residue was washed with deionised water to a neutral pH. The filter paper containing the residue was placed in a previously weighed platinum crucible, dried on a heat plate and calcined at 1000 °C in a furnace for 1 h. The percentage of the dissolved phases was deduced from the weight loss.

The conversion factor or "α" and "IR" or the insoluble residue were determined with Eqs. (1) and (2).

$$\mathrm{IR}(\%) = \frac{P_{\mathrm{final}}}{P_{\mathrm{initial}}} \times 100 \tag{1}$$

$$\alpha(\%) = 100 - \mathrm{IR}(\%) \tag{2}$$

where P_{initial} is the initial weight of the sample; P_{final} is the final weight of the insoluble residue after the HCl attack and calcination at 1000 °C; IR is the unreacted percentage of fly ash (insoluble residue) and α is the percentage of reaction product.

2.2.3. Sample preparation for amorphous quantitative phase analysis

An external standard was added to all the samples in order to carry out the quantification of amorphous content by the

Table 2
Reactive silica content in Compostilla fly ash (%)

	IR[a](KOH+HCl)	S.R.[b]	Total SiO_2	Not reactive SiO_2	Reactive SiO_2
Fly ash	15.56	84.44	53.09	2.65	50.44

[a]IR insoluble residue. [b]S.R. soluble residue.

Table 3
Chemical composition and properties of the working solutions

Solution	Chemical composition (% of oxides)			SiO_2/Na_2O	pH[a]	ρ[b](g/cm^3)	$[OH^-]$[c](M)
	Na_2O	SiO_2	H_2O				
N	7.81	0	92.19	0	13.93	1.27	7.6
W15	8.41	1.62	89.97	0.19	13.83	1.35	8.6
W50	7.84	5.40	86.76	0.69	13.81	1.43	8.5
W84	7.72	9.07	83.21	1.17	14.04	1.57	9.3

[a]Measured with a Metrohm pH meter. [b] Measured with a pycnometer. [c] Titrated with HCl.

Rietveld method. The chosen standard was α-Al_2O_3. To obtain this standard γ-Al_2O_3 (ALFA, 99.997% pure) was ground in an agate ball mill at 200 rpm for 30 min. The solid was then heated at 1500 °C for 6 h in a Pt crucible. The resulting powder was sieved (<0.125 mm) prior to be weighed.

All the samples (original and activated ashes) were mixed with a well known amount of standard as described in [18].

2.3. X-ray powder diffraction data collection

Laboratory XRPD patterns were recorded in a Bragg–Brentano (reflection) X'Pert MPD PRO diffractometer (PANalytical) using CuKα_1 radiation (λ=1.54059 Å), [Ge(111) primary monochromator]. The optics used were a fixed divergence slit (1/2°), a fixed incident anti-scatter slit (1°), a fixed diffracted anti-scatter slit (1/2°) and an X'Celerator RTMS (Real Time Multiple Strip) detector, working in scanning mode with maximum active length. The samples were rotated during data collection at 16 rpm in order to enhance particle statistics. The X-ray tube worked at 45 kV and 35 mA. The data were collected from 10° to 70° (2θ) during ~ 15 min for the original and activated ashes in order to follow activation process. On the other hand, all the artificial mixtures patterns, i.e. ash with α-Al_2O_3, were recorded in the same angular range but during ~ 2 h in order to perform Rietveld QPA, including amorphous content determination.

3. Results

3.1. Mechanical strength

Fig. 1 shows the variation in compressive strength with curing time for the various working systems (12 prisms per test were tested).

At short curing times (8 h), an increase in the soluble silica content (W50 and W84) favoured the development of high mechanical strength in the material (compressive strength>30 MPa), with values of up to double the strength recorded in matrices activated with solutions with a lower silica content (N and W15, ≈ 15 MPa). At slightly longer curing times (20 h), however, a substantial increase was observed in the strength of systems with a lower silica content (N and W15), which equalled or even out-performed the other two systems (compressive strength>40 MPa) in this regard. Longer curing times had a consistently beneficial effect on the mechanical strength of all the matrices studied throughout the six-month duration of the experiment, with final compressive strength values greater than 70 MPa in all cases.

3.2. Selective phase dissolution

As explained in the experimental section, a 1:20 (by volume) HCl attack was used to determine the percentage of reaction product and unreacted fly ash in the material at any given time.

Fig. 2 shows the variation in degree of reaction with curing time for the various working systems. Alpha values were observed to increase with curing time in all the systems studied. One rather striking finding was the lower degree of reaction obtained for system W84 at all ages, despite the high mechanical strength obtained (see Fig. 1). The reasons underlying this behaviour are explained in greater detail below.

3.3. XRD mineralogical analysis. Rietveld quantitative amorphous content determination

X-ray powder diffraction patterns for all the materials studied, including the original fly ash, are shown in Fig. 3. Although fly ash is an essentially vitreous material (see halo recorded for 2Θ=20–35°), it also contains a series of minority crystalline phases such as quartz (SiO_2, JCPDS 05–0492), mullite ($3Al_2O_3.2SiO_2$, JCPDS 15–0776) and magnetite (Fe_3O_4, JCPDS 19–0629). The diffraction pattern changed appreciably after the activation of the original fly ash with the different solutions. It has to be highlighted the shift in the position of the halo attributed to the vitreous phase in the initial ash to slightly higher angular values (2Θ=25–40°). This effect is indicating the formation of an alkaline aluminosilicate gel [17]. The crystalline phases (quartz, mullite and magnetite) detected in the initial material remained apparently unaltered with activation. Other zeolite-type crystalline phases also appeared after activation, which varied depending on the nature of the activating solution used and curing time.

X-ray powder patterns for fly ash samples alkali activated with solution N are given in Fig. 3, upper-left side. These specimens were found to contain zeolite species such as hydrated

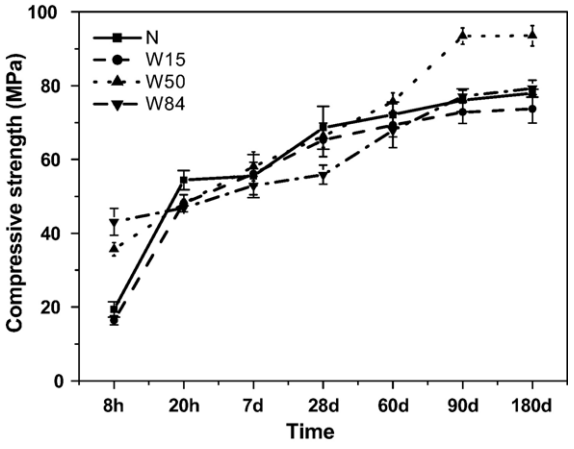

Fig. 1. Mechanical strength vs curing time for the various working systems.

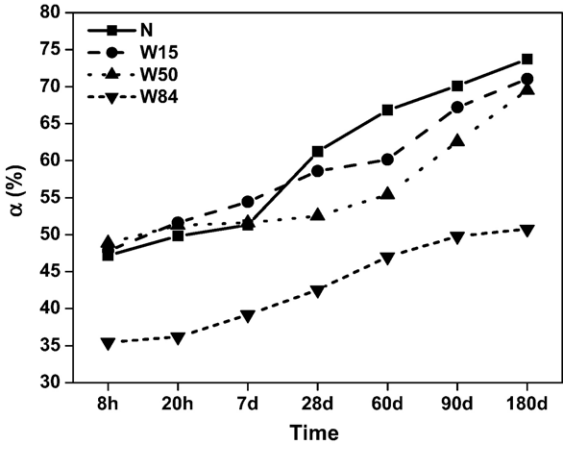

Fig. 2. Conversion factor, "α", vs curing time for the various working systems.

sodalite (also known as hydroxysodalite [20]) ($Na_4Al_3Si_3O_{12}OH$, JCPDS 11–0401) with an Si/Al ratio = 1 and Na-chabazite (also known as herschelite [20]) ($NaAlSi_2O_6 \cdot 3H_2O$, JCPDS 19–1178) with an Si/Al ratio = 2. The amount of hydrated sodalite-type zeolite formed was observed to remain practically unchanged throughout the test, while the Na-chabazite content increased with curing time. Zeolite species such as hydrated sodalite and Na-chabazite were also identified on the W15 patterns, see Fig. 3, upper-right side. Here the amount of hydrated sodalite-type zeolite crystallizing was likewise found to remain constant throughout, while the Na-chabazite-type content grew with curing time (as in the preceding case); the higher proportion of silica in the reaction environment was observed to favour the early crystallization of Na-chabazite (after only 8 h).

X-ray powder patterns for fly ash samples alkali activated with solution W50 are also shown in Fig. 3, bottom-left side. An increase in the soluble silica content in the reaction environment quite clearly induced a delay in the formation of zeolite species. Zeolite Y ($Na_{1.88}Al_2Si_{4.8}O_{13.54} \cdot 9H_2O$, JCPDS 38–0239), with a Si/Al ratio = 2.4, for instance, was not detected until the 28th day of treatment. Moreover, while the amount of this species increased with curing time up to 90 days, after 180 days the predominant zeolite species were Na-chabazite and zeolite P ($Na_{3.6}Al_{3.6}Si_{12.4}O_{32} \cdot 12H_2O$, JCPDS 40–1464) with an Si/Al ratio of 3.4. These changes can be explained by the fact that zeolites are metastable and may undergo successive transformation into one or several more stable phases. Species with a very open structure convert to closed structure zeolites that eventually form analcime (the most stable and densest of

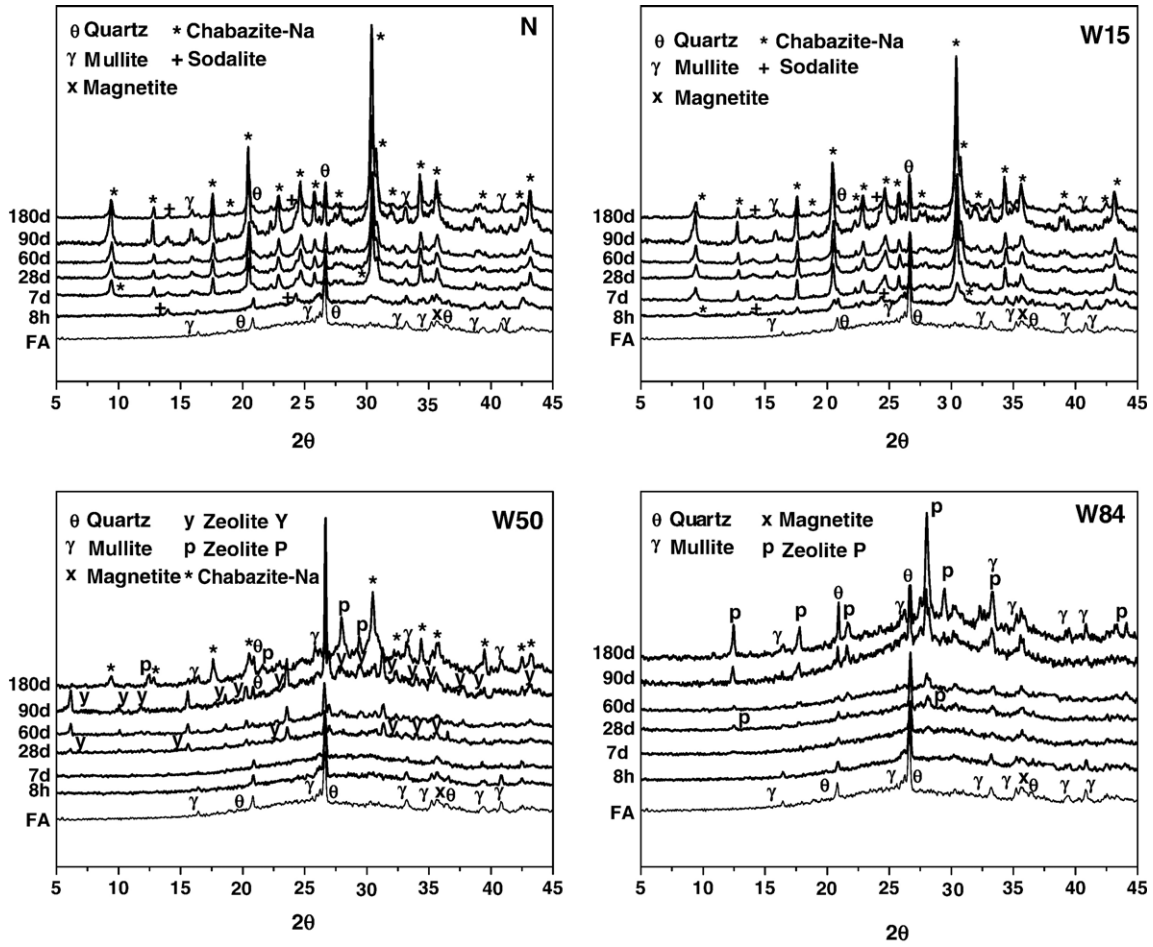

Fig. 3. X-ray powder diffraction patterns of Compostilla fly ash and activated ashes with different alkaline solutions. Main peaks due to a given phase have been labelled.

common zeolites) [5]. The present study yielded similar findings: zeolite Y, a species with a pore size of 0.8 nm, gave way to zeolite P, which has a smaller pore size (0.43 nm) [21] alkali. Finally, X-ray powder patterns for fly ash samples alkali activated with solution W84 are also displayed in Fig. 3, bottom-right side. Here, zeolite P-type phases were observed to be formed. The formation of zeolite species was retarded even further in the presence of the higher silica content in this activating environment than in the preceding solutions. Moreover, zeolite P was not detected until the 28th day, although the content of this crystalline phase grew with curing time.

Rietveld QPA was performed for all the artificial mixtures, original or activated fly ashes with α-Al_2O_3. These results were used to indirectly infer the amorphous content of all the samples, as detailed in [16]. QPA results, including the amorphous content, are given in Table 4. The amorphous fraction of the material stands for the vitreous component of the unreacted fly ash and the sodium aluminosilicate gel which is the first reaction product of alkali activation. Furthermore, in all the samples studied, the percentage of the amorphous phase was observed to decline over time while the zeolite content rose.

The crystal structures used to perform Rietveld refinements were taken from the Inorganic Crystal Structure Database (ICSD). The collection codes for the various structures were: α-Al_2O_3 73725; quartz 63532; mullite 66263; magnetite 30860; calcite 80869; Na-chabazite 201584; sodalite 72059; zeolite Y 201472; zeolite P 9550; cancrinite 32582 and phillipsite 51639. Neither the positional nor the thermal vibration parameters were refined. The parameters optimized were: background coefficients, cell parameters, zero-shift error, peak shape parameters (including anisotropic terms if needed), and phase fractions.

A selected range of the Rietveld plot for the initial fly ash mixed with α-Al_2O_3 is given in Fig. 4(A), where main peaks due to a given phase have been labelled. The same selected range of the Rietveld plots for the mixture of activated fly ash treated with W15 solution after a reaction time of 8 h with the standard and the activated fly ash treated with W84 after 90 days with standard are given in Fig. 4(B) and (C) respectively.

4. Discussion

The alkali activation of fly ash is a chemical process in which the vitreous structure of most of its particles is converted into a compact cementitious skeleton [2,22,23]. Earlier studies [4,17,24] showed that the main reaction product of the alkali activation of fly ash is a sodium aluminosilicate gel. This aluminosilicate exhibits long- and medium-range disorder, making it amorphous to X-ray diffraction, but at the nanometric level it is found to have a zeolite-type three-dimensional structure [4]. One of the most ambitious objectives pursued by researchers (in any line of work) has traditionally been not only to quantitatively monitor but to obtain quantitative control over the chemical reactions involved in the formation of the desired products. In the case of the generation of new cementitious

Table 4
Rietveld quantitative phase analysis, including amorphous content, of the initial (Compostilla) and activated fly ash

Sample	Amorphous[a]	Mullite	Quartz	Magnetite	Calcite	Zeolite					
						Na-chabazite	Cancrinite	Sodalite	Y	P	Phillipsite
Fly ash	83.4[b]	7.0	8.2	1.4							
N8h	86.8	3.8	3.9	0.6		2.1	0.8	2.0			
N7d	71.4	1.6	1.5	0.7		22.2	1.3	1.3			
N28d	68.5	1.5	1.2	0.7		25.7	1.3	1.1			
N60d	65.0	1.6	1.3	0.6		29.4	1.3	0.8			
N90d	60.7	1.5	1.4	0.7		33.7	1.3	0.7			
N180d	57.1	3.2	2.6	0.6		34.2	1.4	0.9			
W158h	78.1	5.7	4.5	0.7		9.9		1.1			
W157d	66.0	1.7	1.4	0.9		27.3	1.1	1.6			
W1528d	63.0	1.7	1.4	0.9		30.0	1.2	1.8			
W1560d	63.7	1.8	1.2	1.0		29.4	1.3	1.6			
W1590d	57.8	3.5	1.8	0.9		33.9	1.3	0.8			
W15180d	55.4	3.4	2.0	0.7		36.8	0.9	0.8			
W508h	91.2	4.7	3.1	1.0							
W507d	96.0	1.6	1.6	0.8							
W5028d	91.0	1.0	1.5	0.7					5.7		
W5060d	89.1	1.0	2.1	0.7					7.1		
W5090d	88.8	0.6	1.7	0.6					8.3		
W50180d	80.9	2.3	1.5	0.8		2.3				2.0	10.1
W848h	91.9	3.6	4.0	0.4							
W847d	96.5	1.4	1.8	0.4							
W8428d	95.3	1.0	1.4	0.4						1.1	0.7
W8460d	93.0	1.2	1.5	0.4						2.3	1.6
W8490d	86.2	1.9	1.0	0.6	1.0					6.1	3.2
W84180d	83.1	2.3	1.5	0.8	1.2					6.7	4.4

[a] Amorphous = vitreous phase in the initial ash + sodium aluminosilicate gel (primary reaction product in alkali activation).
[b] Amorphous = vitreous phase in the initial ash.

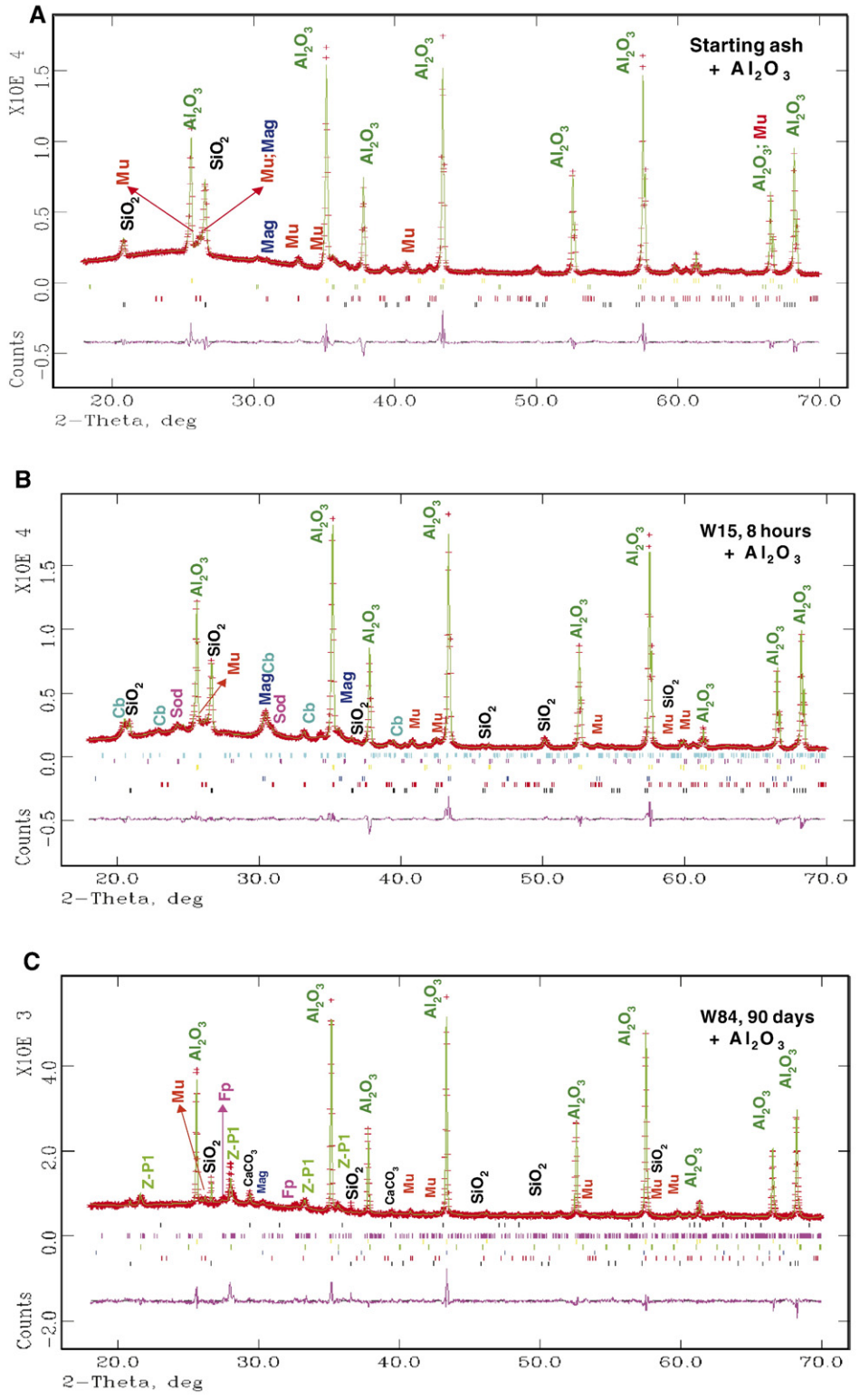

Fig. 4. Selected range of the Rietveld plots for the mixtures of α-Al_2O_3 with A) original fly ash; B) activated fly ash with W15 solution (8 h); C) activated fly ash with W84 solution (90 days). Mu: mullite; Mag: magnetite; Sod: sodalite; Cb: Na-chabazite; Z-Pl: zeolite P; Fp: phillipsite.

materials (zeocements or zeoceramics) through the alkali activation of aluminosilicates, this objective has been met by attacking these materials with hydrochloric acid [18,19,25]. A step forward in the relevant research prompted the authors of the present paper to quantitatively correlate the type of system studied (with a higher or lower soluble silica content) with the amount of cementitious gel generated and the mechanical properties acquired by the material in response to gel content. An attack with 1:20 (by volume) HCl dissolves the reaction products. Consequently, the results obtained from that attack

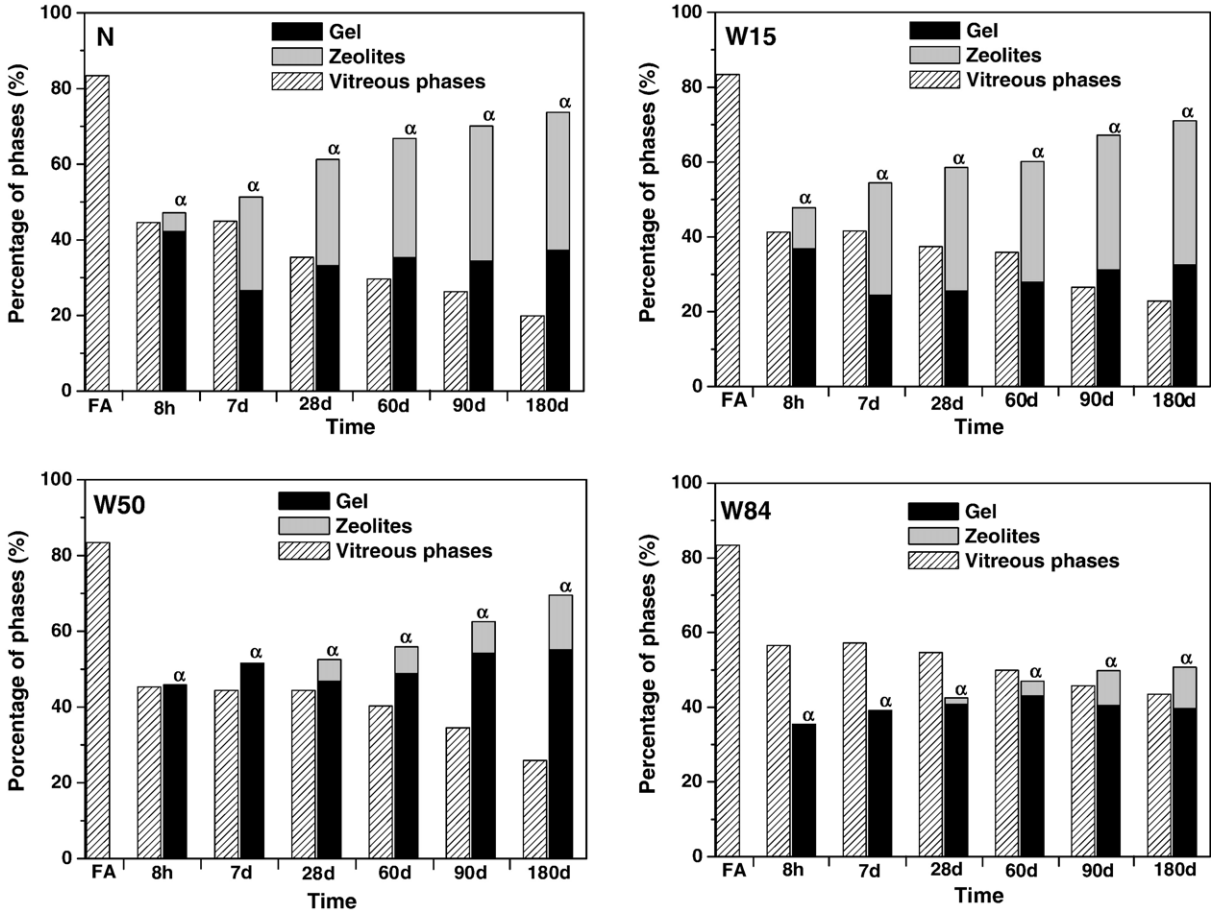

Fig. 5. Percentage of the different phases comprising the initial and the alkali activated ashes.

(see Fig. 2), in conjunction with Rietveld QPA results, can be substituted into Eqs. (3) and (4) to determine the percentage of the vitreous phase still present (Glass), as well as the amount of zeolites (Z) and sodium aluminosilicate gel (Gel) in each of the materials studied.

$$\alpha(\%) = \mathrm{Gel}(\%) + \mathrm{Z}(\%) \tag{3}$$

$$\mathrm{IR}(\%) = \mathrm{Glass}(\%) + \mathrm{Mu}(\%) + \mathrm{Q}(\%) + \mathrm{Fe}(\%) \tag{4}$$

Where α is the conversion factor (% of material dissolved in the 1:20 HCl); Gel is the per cent of sodium aluminosilicate gel and Z the percentage of zeolites (calculated with the Rietveld method, see Table 4).

IR, in turn, stands for the insoluble residue in 1:20 HCl (% insoluble phase, see Fig. 2); Glass is the percentage of unreacted vitreous phase; Mu is the percentage of mullite; Q is the percentage of quartz and Fe is the percentage of magnetite (all found with Rietveld methodology, see Table 4).

Fig. 5 shows the variation over time in conversion factor α (i.e., gel plus zeolites), and vitreous phases present in the initial ash for each and every one of the working systems. The amount of vitreous phase present in the initial ash declined substantially with increasing reaction time in all the systems, since this was the phase that feeds the activation reactions. This decline tapered with time in systems W50 and W84; this is pointing out that when soluble silica is highly polymerized, as in the case of solutions W50 and W84 (see Fig. 6) [26], ash dissolution takes place more slowly due to large saturation of the ionic silica species.

As mentioned above, the conversion factor α, at any given time is closely related to the amount of gel and zeolites forming in the activated ash. An analysis of the variation in the two phases (gel and zeolites) in each system studied reveals that the percentage of zeolites always grows at the expense of the percentage of gel (see Fig. 5). In other words, this may provide confirmation of the hypothesis long sustained that the sodium aluminosilicate gel is a zeolite precursor [27] with a thermodynamic tendency, therefore, to crystallize into a zeolite.

Moreover, the highest initial and final mechanical strengths (see Fig. 1) were consistently obtained with the systems having higher soluble silica content (W50 and W84). That means that the delay in the initial dissolution of the ash (see Fig. 2) observed in systems with high percentages of soluble silica and the concomitant deceleration of activation kinetics are offset by the formation of large molecular species and consequently a denser, more compact and stronger gel [28]. It might also be reasonably assumed that the energy needed to reorganize these molecules into nanocrystals must be much greater than in

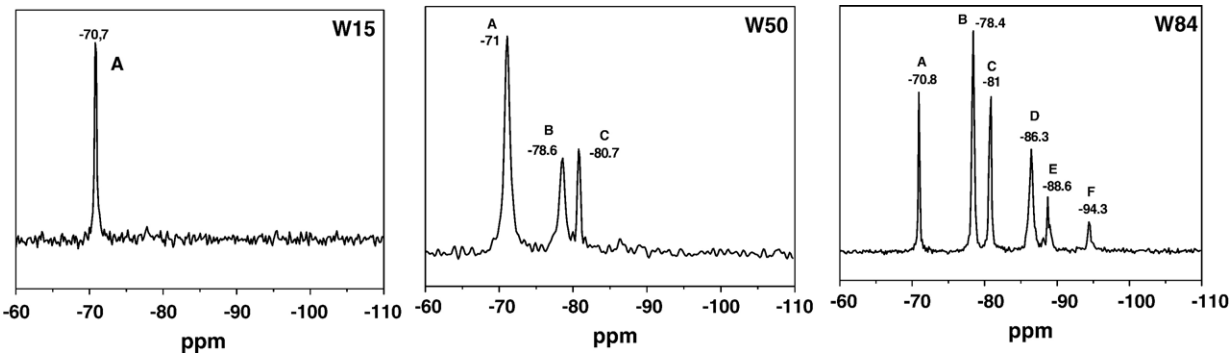

Fig. 6. ^{29}Si MAS NMR spectra of the liquid activation solutions.

systems N and W15 and that therefore the amount of zeolites forming in the systems containing a high soluble silica content is much smaller than the amount generated in the other two systems (see Table 4 and Fig. 5).

Systems N and W15 were observed to contain the same zeolites: cancrinite ($(Na_2O)_{1.3}Al_2O_3(SiO_2)_{2.01}(H_2O)_{1.65}$, JCPDS 75–2318) (not labelled in the patterns in Fig. 3 due to its low percentage), sodalite and Na-chabazite. A small amount of monomeric silica (see Fig. 6) has no effect on the type of zeolite formed, although it does hasten reaction kinetics (system W15 favours the crystallization of Na-chabazite, the most stable and predominant species under these working conditions). While cancrinite and sodalite form readily under favourable local conditions (in terms of alkalinity and composition), their subsequent crystalline formation or growth is prevented because of the unpropitious conditions (particularly as regards composition) prevailing in the system as an other [6]. In the two matrices with an abundance of soluble silica and a higher degree of polymerization, different zeolite species form. Logically, the percentage of zeolites in these systems also grows with time. The amount of zeolite Y, detected in system W50 after 28 days, rises up to a reaction time of 90 days and then disappears, giving way to Na-chabazite, zeolite P and phillipsite ($(K,Na)_2(Si,Al)_8O_{16}4H_2O$, JCPDS 46–1427) (not labelled on the diffractograms in Fig. 3 because the amount is very small and the respective diffraction peaks may overlap with the zeolite P peaks), the species that prevail after 180 days. The zeolite species that crystallize in system W84 after 28 days are zeolite P and phillipsite; the percentage of these zeolites rises with reaction time (see Table 4).

Rietveld quantitative analysis reveals that the crystalline phases in the initial ash (quartz, mullite, magnetite) are not as inalterable as the findings of prior studies [24,29,30], but rather undergo minor alterations during the activation process. Table 4 gives the quartz, mullite and magnetite content for all the samples. These results show that while the percentage of quartz and mullite declined, magnetite did not appear to be impacted by the alkaline attack.

These data suggest that the aggressive conditions required for the reaction to take place affected both quartz and mullite, albeit slightly. This observation in fact concurs with prior findings [31], in which a scanning electron microscopic study detected alterations on the surface of mullite crystals.

Finally, Fig. 7 shows the variation in both mechanical strength (A) and the amount of gel formed (B) in terms of the percentage of soluble silica added. Higher strength values were found at all reaction times for system W50, which was, in turn, the system with the highest percentage of gel (see Fig. 7), followed by systems W84, N and W15 in descending order. The low level of reactivity correlated with high strength in W84 series may confirm the hypothesis of P. Duxson et al., J. Provis et al. [32] by which mechanical strength is likely to be derived from contributions from gel and "aggregated" materials.

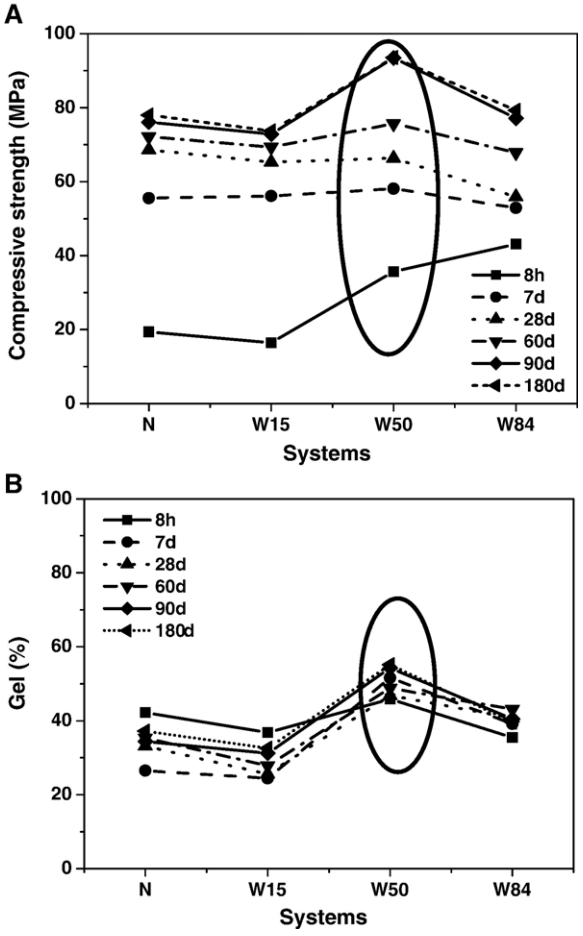

Fig. 7. Variation in mechanical strength (A) and amount of gel formed (B) versus the percentage of soluble silica added.

Results show that the mechanical strength development of these types of materials depends not only on the reaction degree (see Fig. 2) but also on the nature and composition of the reaction products, the aluminosilicate gel being the main product of reaction inducing the mechanical properties. The higher the amount of this "prezeolite", the higher the mechanical strength (see Fig. 7). On the other hand, a high content of crystalline zeolites prevents the high mechanical strength development. This is the reason why systems N and W15, although having a high conversion factor, develop lower mechanical strength than system W50.

5. Conclusions

- Upon activation the amount of vitreous phase present in the initial fly ash declines with time, since this is the phase that essentially feeds the activation reaction.
- The material owes its good mechanical performance primarily to the sodium aluminosilicate gel.
- Zeolites are formed as secondary reaction products. At the present curing temperature of 85 °C the percentage of zeolites increases with curing time at the expense of the percentage of gel. The inclusion of a greater amount of soluble silica in the environment retards zeolite formation, mainly due to the higher degree of polymerization of such silica. Consequently, systems W50 and W84 had higher gel content than systems N and W15.
- The amount of quartz and mullite slightly declines at longer reaction times. These phases are partially attacked under the aggressive conditions prevailing in such reactions.

Acknowledgements

This study was funded by the Directorate General of Scientific Research (project BIA2004–04835). The Spanish Council for Scientific Research (CSIC) and the European Social Fund co-financed a 13P-PC2004L contract in connection with this study. The authors wish to thank J. García and A. Gil for their assistance in the preparation of the specimens.

References

[1] V.D. Glukhovshy, Soil silicates, Gosstroy publsh, Kiev (Ukraine), 1959.
[2] A. Palomo, M.W. Grutzeck, M.T. Blanco, Alkali-activated fly ashes. A cement for the future, Cem. Concr. Res. 29 (1999) 1323–1329.
[3] A. Fernández-Jiménez, A. Palomo, M. Criado, Microstructure development of alkali-activated fly ash cement: a descriptive model, Cem. Concr. Res. 35 (2005) 1204–1209.
[4] A. Palomo, S. Alonso, A. Fernández-Jiménez, I. Sobrados, J. Sanz, Alkaline activation of fly ashes: NMR study of the reaction products, J. Am. Ceram. Soc. 87 (2004) 1141–1145.
[5] A. Dyer "An introduction to zeolite molecular sieves", Ed. Wiley New York (USA), 1988.
[6] F.R. Ribeiro, A.E. Rodrigues, L.D. Rollmann, C. Naccade, Synthesis of zeolites: an overview, Zeolites: Science and Techology, Ed. NATO ASI Series 80 Holand 1984 109–147.
[7] M. Criado, A. Fernández-Jiménez, A. Palomo, Alkali Activation of fly ash. Effect of the SiO_2/Na_2O ratio. Part I: FTIR study, Microp. Mesop. Mat. (submitted for publication).
[8] M. Paul, Application of the Rietveld method in the cement industry, Microstructure Analysis in Materials Science Freiberg (Germany), 2005.
[9] N.V.Y. Scarlett, I.C. Madsen, L.M.D. Cranswick, T. Lwin, E. Groleau, G. Stephenson, M. Aylmore, N. Agron-Olshina, Outcomes of the international union of crystallography commission on powder diffraction round robin on quantitative phase analysis: samples 2, 3, 4, synthetic bauxite, natural granodiorite and pharmaceuticals, J. Appl. Crystallogr. 35 (2002) 383–400.
[10] A.G. de la Torre, A. Cabeza, A. Calvente, S. Bruque, M.A.G. Aranda, Full phase analysis of Portland clinker by penetrating synchrotron powder diffraction, Anal. Chem. 73 (2001) 151–156.
[11] A.G. de la Torre, M.A.G. Aranda, Accuracy in Rietveld quantitative phase analysis of Portland cements, J. Appl. Crystallogr. 36 (2003) 1169–1176.
[12] I. Pajares, A.G. De la Torre, S. Martínez-Ramírez, F. Puertas, M.T. Blanco-Varela, M.A.G. Aranda, Quantitative analysis of mineralized white Portland clinkers: The structure of Fluorellestadite, Powder Diffr. 17 (2002) 281–286.
[13] A.H. De Aza, A.G. De la Torre, M.A.G. Aranda, F.J. Valle, S. De Aza, Rietveld quantitative analysis of Buen Retiro porcelains, J. Am. Ceram. Soc. 87 (2004) 449–454.
[14] I. Juel, E. Jons, The influence of earth alkalis on the mineralogy in a mineralized Portland cement clinker, Cem. Concr. Res. 31 (2001) 893–897.
[15] S.J. Barnett, C.D. Adam, A.R.W. Jackson, P.D. Hywel-Evans, Identification and characterisation of thaumasite by XRPD techniques, Cem. Concr. Compos. 21 (1999) 123–128.
[16] A.G. De la Torre, S. Bruque, M.A.G. Aranda, Rietveld quantitative amorphous content analysis, J. Appl. Crystallogr. 34 (2001) 196–202.
[17] A. Fernández-Jiménez, A. Palomo, Characterisation of fly ashes. Potential reactivity as alkaline cements, Fuel 82 (2003) 2259–2265.
[18] A. Fernández-Jiménez, A.G. de la Torre, A. Palomo, G. López-Olmo, M.M. Alonso, M.A.G. Aranda, Quantitative determination of phases in the alkali activation of fly ash. Part I. Potential ash reactivity, Fuel 85 (2006) 625–634.
[19] A. Fernández-Jiménez, A.G. de la Torre, A. Palomo, G. López-Olmo, M.M. Alonso, M.A.G. Aranda, Quantitative determination of phases in the alkali activation of fly ash. Part II. Degree of reaction, Fuel 85 (2006) 1960–1969.
[20] D.W. Breck, Zeolite molecular sieves, Ed. Krieger Florida (USA), 1973.
[21] H.V. Bekkum, E.M. Flanigen, P.A. Jacobs, J.C. Jansen, Introduction to zeolite science and practice, Studies in Surface Science and Catalysis, Ed. Elsevier Science BV 137 Amsterdam (Holland) 2001.
[22] P. Krivenko, Alkaline cements: terminology, classification, aspects of durability, performance and durability of cementitious materials, in: H. Justnes (Ed.), Proc. of 10th Int. Cong. Chem. Cem.(ICCC), 1997, vol. 4 Gothebburg (Sweden).
[23] A. Fernández-Jiménez, A. Palomo, Alkali activated fly ashes: properties and characteristics, in: G. Grieve, G. Owens (Eds.), Proc. of 11th Int. Cong. Chem. Cem. (ICCC) vol. 3 Durban (South Africa), 2003, pp. 1322–1340.
[24] A. Fernández-Jiménez, A. Palomo, Composition and microstructure of alkali activated fly ash binder: effect of the activator, Cem. Concr. Res. 35 (2005) 1984–1992.
[25] M.L. Granizo, S. Alonso, M.T. Blanco-Varela, A. Palomo, Alkaline activation of metakaolin: effect of calcium hydroxide in the products of reaction, J. Am. Ceram. Soc. 85 (2002) 225–231.
[26] G. Engelhardt, D. Michel "High Resolution Solid State NMR of silicates and zeolite", Ed. Wiley, (1987), London, UK.
[27] A. Palomo, F.P. Glasser, Chemically-bonded cementitious materials based on metakaolin, Br. Ceram., Trans. J. 91 (1992) 107–112.
[28] A. Fernández-Jiménez, A. Palomo, I. Sobrados, J. Sanz, The role played by the reactive alumina content in the alkaline activation fly ashes, Microp. Mesop. Mat. 91 (2006) 111–119.
[29] Z. Xie, Y. Xi, Hardening mechanisms of an alkaline-activated class F fly ash, Cem. Concr. Res. 31 (2001) 1245–1249.
[30] A. Molina, C. Poole, A comparative study using two methods to produce zeolites from fly ash, Miner. Eng. 17 (2004) 167–173.
[31] A. Palomo, A. Fernández-Jiménez, M. Criado, "Geopolymers": same basic chemistry, different microstructures, Mater. Constr. 54 (2004) 77–91.
[32] P. Duxson, J.L. Provis, G.C. Lukey, S.W. Mallicoat, W.M. Kriven, J.S.J. van Deventer, Understanding the relationship between geopolymer composition, microstructure and mechanical properties, Colloids Surf., A 269 (2005) 47–58.